Anomalous Scaling and Solitary Waves in Systems with Non-Linear Diffusion

Alex Hansen,* Bo-Sture Skagerstam,† and Glenn Tørå‡
Department of Physics, Norwegian University of Science and Technology, N–7491 Trondheim, Norway

We study a non-linear convective-diffusive equation, local in space and time, which has its background in the dynamics of the thickness of a wetting film. The presence of a non-linear diffusion predicts the existence of fronts as well as shock fronts. Despite the absence of memory effects, solutions in the case of pure non-linear diffusion exhibit an anomalous sub-diffusive scaling. Due to a balance between non-linear diffusion and convection we, in particular, show that solitary waves appear. For large times they merge into a single solitary wave exhibiting a topological stability. Even though our results concern a specific equation, numerical simulations supports the view that anomalous diffusion and the solitary waves disclosed will be general features in such non-linear convective-diffusive dynamics.

PACS numbers: 47.20.Ft,47.56.+r,47.54.-r,89.75.Fb

Anomalous diffusion is a topic of great current interest (see e.g. Refs. [1–3]). It is commonly believed that the phenomenon has its roots in correlated structures and/or disorder in the medium in which the diffusion occurs which, in turn, induce memory effects. However, it is the aim of the present work to demonstrate that a non-linearity in the diffusion process, local in space and time, is sufficient to induce anomalous scaling. When, in addition, convection enters the non-linear diffusion problem we consider, we find, in particular, that the same non-linearities that cause the anomalous diffusion, also lead to the occurrence of solitary waves exhibiting a topological stability. The topological stability manifests itself through the solitary waves having their speed given by their average amplitude.

Even though the non-linear diffusion-convection equation that we study has its origins in the dynamics of wetting films, related equations appear in other context like non-linear heat conduction [4, 5]. Wetting films have, in their own right, received much attention recently due to their relevance for flows in porous media (see e.g. Refs.[6]) and soil physics and hydrology [7]. Shock-wave features are in general expected in systems with non-linear convection and diffusion [8]. In elastic media such features has recently been observed in the laboratory [9]. Due to the generic non-linearities in the equations of motion an exact mathematical analysis is often not possible and numerical simulations are then expected to be mandatory. The lack of an exact mathematical analysis may, however, prevent one from a deeper insight into the physical consequences of the non-linear dynamics.

In order to be specific, we consider a capillary pore flow with a wetting film flowing in a closed wedge with a length L as illustrated in Fig.1 The geometry chosen appears not be essential but enables us to derive specific and analytical predictions. We denote the position along the wedge with x such that $0 \leq x \leq L$, and where, e.g., the endpoints could be connected to other pores. For reasons of simplicity we will consider an infinite half-line and hence make L arbitrarily large. The cross sectional area of the film at x is $a \equiv a(x,t)$, where $t \geq 0$ is the time variable. The total and fixed cross sectional area of the wedge is A_T so that the remaining cross section is $\delta A(x,t) = A_T - a$. Apart from the wetting film, the closed wedge is filled with a non-wetting fluid. There is a pressure drop $P \equiv P(x,t)$ along the wedge in the non-wetting fluid and a pressure drop $p \equiv p(x,t)$ in the wetting film. The non-wetting fluid flows with a volume flow rate $Q \equiv Q(x,t)$ and the wetting fluid with a volume flow rate $q \equiv q(x,t)$ so that the total $Q_T = Q + q$ is constant. Both fluids are assumed to be incompressible. The non-wetting fluid has a viscosity M and the wetting fluid a viscosity μ.

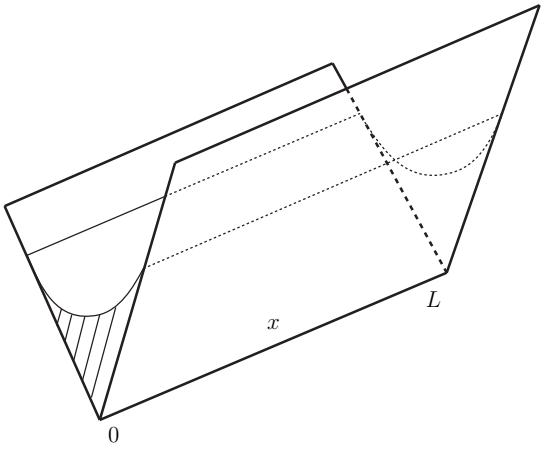

Figure 1: Flow of a wetting film in a wedge. The shaded area denotes a cross-section area $a(x,t)$ of the film which, in general, various along the wedge.

Conservation of mass dictates that the area a is related to the flow rate through the equation

$$\frac{\partial q}{\partial x} + \frac{\partial a}{\partial t} = 0 \, . \tag{1}$$

We consider a flow in the films governed by the Darcy

*Alex.Hansen@ntnu.no
†Bo-Sture.Skagerstam@ntnu.no
‡Glenn.Tora@ntnu.no

equation [10], i.e.

$$q = -\frac{k(a)}{\mu}\,\frac{\partial p}{\partial x}\,. \tag{2}$$

Here $k(a) = a^2/8\pi$ is the effective and a-dependent film permeability of the film, assuming a Hagen-Poiseuille flow [10]. The Young relation now gives the connection between pressure difference across the interface between wetting and non-wetting fluids and the curvature of the interface r at capillary equilibrium [10], i.e. $P - p = \gamma/r$, where γ is the surface tension. If the wedge has an opening angle ϕ and the wetting angle is zero, then a geometrical consideration leads to $a = r^2\,(\cot(\phi/2) - \phi/2)$. Combining this relation with the Young relation leads to

$$p = P - \frac{\overline{\gamma}}{\sqrt{a}}\ , \tag{3}$$

where we have defined the effective surface tension $\overline{\gamma} = \gamma\sqrt{a}/r$. If we now eliminate p and q between Eqs. (1) – (3), we find our basic equation of motion

$$\frac{\partial}{\partial x}\left[a^2\,\frac{\partial}{\partial x}\left(P - \frac{\overline{\gamma}}{\sqrt{a}}\right)\right] = 8\pi\mu\,\frac{\partial a}{\partial t}\,. \tag{4}$$

We now make the assumption that the pressure in the non-wetting fluid, P, is unaffected by the area a of the film. This is true if $\delta A >> a$. The Darcy equation (2) then reads $MQ/K = -\partial P/\partial x$, where $K = A_T^2/8\pi$ is the effective permeability of an assumed Hagen-Poiseuille bulk flow. Due to conservation of mass of the non-wetting fluid we have $\partial Q/\partial x = 0$, which, after a straightforward integration, leads to

$$\frac{\partial P(x,t)}{\partial x} = -\frac{8M\pi\bar{Q}}{A_T^2}\,, \tag{5}$$

where the pressure drop at $x = 0$ is neglected, i.e., $\partial P(0,t)/\partial x = 0$, and $\bar{Q} \simeq Q > 0$ is a characteristic volume flow rate. All time dependencies enter through the non-wetting pressure P at $x = 0$. If there is no flow of non-wetting fluid in the pore, $Q = 0$, the pressure P is constant along it.

The two fundamental equations in the present paper for the evolution of the film in the wedge are Eqs. (4) and (5). We non-dimensionalize and combine them by setting $a = \bar{a}\alpha$, $x = \bar{x}\xi$ and $t = \bar{\tau}\tau$, where $\bar{a}, \bar{x}, \bar{\tau}$ are some typical area, length and time-scales. The combined equation is the *diffusion-convection equation*

$$\frac{\partial}{\partial\xi}\left(\,w\sqrt{\alpha}\frac{\partial\alpha}{\partial\xi}\right) - v\alpha\frac{\partial\alpha}{\partial\xi} = \frac{\partial\alpha}{\partial\tau}\,. \tag{6}$$

where $w = \bar{a}^{1/2}\bar{\tau}\overline{\gamma}/(16\pi\mu\bar{x}^2)$ and $v = 2M\bar{a}\bar{\tau}\bar{Q}M/(A_T^2\bar{x}\mu)$ can be regarded to be the relevant physical parameters in the system. The diffusivity in Eq. (6) is $D = w\sqrt{\alpha}$ and there is also a convective flow velocity $v\alpha$ both of which therefore are now non-trivial functions of a.

The effective diffusivity $D = w\sqrt{\alpha}$ is counter intuitive when interpreting the diffusion process literary: The diffusion coefficient increases with increasing concentration contrary to conventional diffusion where higher concentration means a more crowded system and, hence, slower diffusion. The non-linear convective term $v\alpha\partial\alpha/\partial\xi$ in Eq. (6) is well known from surface wave propagation in shallow water (see e.g. Ref. [8]). It corresponds to a wave moving towards increasing ξ with a speed proportional to α. In the context of shallow-water theory, it is the term that produces breaking waves: An initially smooth wave will eventually produce a singularity at the leading side.

When there is no non-wetting fluid flow, only the diffusive term is present on the left hand side of Eq. (6). Eq. (6) without convection was considered Ref.[11] as a model for experimental results of imbibition processes. The experimental presence of an imbibition front was theoretically inferred using approximative solutions of Eq. (6) [5]. Here we point out the existence of such fronts as well as shock fronts as exact consequences of Eq. (6). It is also a remarkable consequence of our analysis that anomalous scaling laws of the form $\xi^2 \simeq t^\gamma$ with $\gamma \neq 1$ can be obtained without invoking fractional derivatives [2] in diffusion-like equations (see e.g. Refs. [3]) or by referring to stochastic Mori-Lee equations [12] and memory effects (see e.g. Refs. [13, 14]). If the effective diffusivity D is an increasing (or decreasing) function of α we find sub-diffusion with $\gamma < 1$ (or super-diffusion with $\gamma > 1$). A related observation of the appearance of anomalous diffusion in a class of non-linear Fokker-Planck equations can be found in Ref.[15]. A renormalization group analysis of the so called Barenblatt's non-linear diffusion equation without convection, which describes the filtration of a certain compressible fluid through an elastic porous medium, also leads to anomalous diffusion [16]. The diffusive non-linearity has then, however, a completely different origin and form as compared to the non-linearities considered in the present paper.

The non-linear diffusion equation obtained from Eq. (6) with $v = 0$ can now be transformed from a partial differential equation to an ordinary one in terms of a scaling function h such that $\alpha(\xi,\tau) = h\,(\xi/f(\tau))\,/f(\tau)$. This choice of scaling of the solution is not unique but is, by construction, such that a load E defined as $E = \int_0^{L/\bar{x}} d\xi\alpha(\xi,\tau)$ is conserved in time provided it is finite. We now obtain

$$h_0 = \sqrt{h}\,\frac{dh}{dy} + cyh\,. \tag{7}$$

as well as

$$f(\tau) = (1 + \frac{5cw\tau}{2})^{2/5}\,, \tag{8}$$

in terms of two constants, h_0 and c, of integration. Here we have defined the natural Boltzmann scaling variable $y = \xi/f(\tau)$ [17]. We notice that the scaling form of the solution and Eq. (8) leads to anomalous scaling since $h \simeq$ *constant* corresponds to $\xi^2 \simeq \tau^{4/5}$, i.e. sub-diffusion,

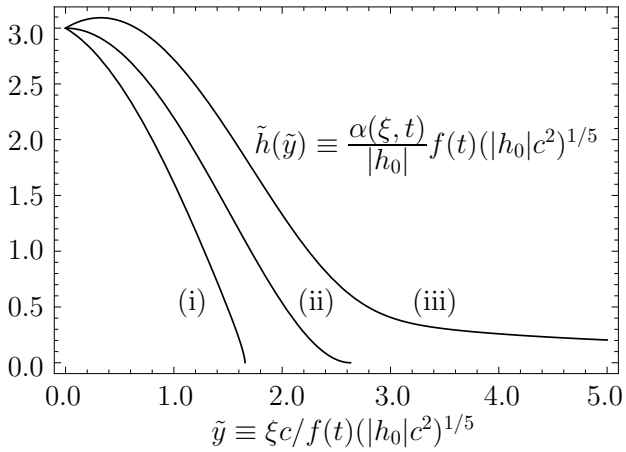

Figure 2: Summarizing, with $\tilde{h}(0) = 3$, the three branches of the integral curves Eq. (10) with $k = -1$ (curve (i) with a shock front), and $k = 1$ (curve (iii) with a front). In the case $k = 0$ (curve (ii)) we make the replacement $|h_0| \to \tilde{h}(0)^{5/4}$.

and that solutions of the scaling form $\alpha(\xi,\tau) = h\left(\xi/g(\tau)\right)$ lead to the conventional scaling $g(\tau) \simeq \tau^{1/2}$. The constant of integration h_0 in Eq. (7) can have either sign. The constant $c > 0$ can be determined from a condition on $\partial\alpha(\xi,\tau)/\partial\tau$ at $\tau = 0$ or by the load E. As long as $h_0 \neq 0$ we can now write the solution $\alpha(\xi,\tau)$ in the form

$$\alpha(\xi,\tau) = \frac{|h_0|}{(|h_0|c^2)^{1/5} f(t)} \tilde{h}(\tilde{y}) \ , \tag{9}$$

where we have defined $\tilde{y} = \xi c/(|h_0|c^2)^{1/5} f(\tau)$ and where $\tilde{h} \equiv \tilde{h}(\tilde{y})$ now obeys the equation

$$k = \sqrt{\tilde{h}}\ \frac{d\tilde{h}}{d\tilde{y}} + \tilde{y}\tilde{h} \ , \tag{10}$$

with $k = h_0/|h_0| = \pm 1$. The scale transformations $\xi \to \lambda\xi; \tau \to \lambda^2\tau; c \to c/\lambda^2$ and $|h_0| \to |h_0|/\lambda$ leaves $\tilde{y}$ and $\tilde{h}$ invariant and hence also all solutions $\alpha(\xi,\tau)$ in the form as given by Eq. (9). Let us now assume that the film is concentrated initially around the origin, $\xi = 0$. Hence, $d\alpha/dy < 0$, and we must have that $k = -1$. Eq. (10) then shows that the solution $\tilde{h}$ flows towards $\tilde{h}(y_{\max}) = 0$ at some finite value $y = y_{\max}$ with an infinite derivative, i.e. we have a shock front. Even though we do not, at present, have an analytical result for $y_{\max}$ given $\tilde{h}(0)$, one can easily calculate $y_{\max}$ numerically. We then find that $y_{\max} \simeq \log \tilde{h}(0)$, at least for large values of $\tilde{h}(0)$. Since $y_{\max}$ is finite the load E will also be finite, which then leads to a possible determination of c in terms of E. If, on the other hand, $k = 1$ we find, using Eq. (10), that $\tilde{h}$ will have a maximum and then flows to zero asymptotically according to $\tilde{h} \simeq 1/\tilde{y}$. In this case the load E is not well defined and the constant of integration c can then be determined using initial data as mentioned above. Finally, we have to consider the special case with $k = 0$ in Eq. (10) which then can be solved explicitly. In the scaling variable $\tilde{y}$ one then makes the replacement $|h_0| \to \tilde{h}(0)^{5/4}$ and we can then write

$$\alpha(\xi,\tau) = \frac{\alpha_0}{f(t)} \left(1 - \frac{\xi^2 c}{4 f(\tau) \alpha_0^{1/2}}\right)^2 \ , \tag{11}$$

where $\alpha_0 \equiv \alpha(0,0)$. In this case the constant of integration c can, e.g., be determined by the conserved load E. In passing, we notice that the exact solution Eq. (11) corresponds to the known Zeldovich-Raizer solution in the context of non-linear heat conduction [4, 5]. We show the various scaling solutions $\tilde{h}(\tilde{y})$ of Eq. (10) graphically in Fig. 2 for a specific initial value. As we have shown above the solutions with $k = -1$ and $k = 0$ have then a finite range. All solutions exhibits anomalous scaling due to Eq. (8).

We will now turn to the existence of solitary wave propagation in the pore. In the following we solve the film equation Eq. (6) under the assumption that the system is infinitely long. Hence, we make a shift of the origin $x = 0$ and let $L \to \infty$ so that ξ can take any value on $(-\infty, +\infty)$. Intuitively, when, in a non-linear system, the convective term is non-zero, there may be propagating solutions where the convective term and the diffusive terms balance each other as is the case for the Burgers equation [8]. The dynamical equation we consider, i.e. Eq.(6), actually has the same convective term as the Burgers equation but describes the diffusion in a non-linear manner. In our case, the primary physical reason for the balance alluded to above therefore is the effective diffusion constant which is proportional to $\sqrt{\alpha}$ and hence increases the diffusion rate with increasing α.

By defining the natural variable $z = \xi - U\tau$ with $U > 0$, then, after an integration, Eq. (6) is transformed into

$$K = w\sqrt{\alpha}\ \left(\frac{d\alpha}{dz}\right) - \left(\frac{v}{2}\right)\ \alpha^2 + U\ \alpha \ , \tag{12}$$

where K is an integration constant. We now rewrite this equation in the form

$$\frac{\sqrt{\alpha}}{(\alpha - \alpha_+)(\alpha - \alpha_-)} \frac{d\alpha}{dz} = \frac{v}{2w} \ , \tag{13}$$

where we notice that $\alpha_+\alpha_- = 2K/v$ and that the velocity U of the solitary wave is given by

$$\alpha_+ + \alpha_- = \frac{2U}{v} \ , \tag{14}$$

i.e.,

$$\alpha_\pm = \left(\frac{U}{v}\right)\ \left(1 \pm \sqrt{1 - \frac{2Kv}{U^2}}\right) \ . \tag{15}$$

We now search for solitary like solutions $\alpha_s \equiv \alpha$ to Eq. (13) whose variations are localized in space, i.e., $d\alpha_s/d\xi \to 0$ as $|\xi|$ becomes large or, equivalently in

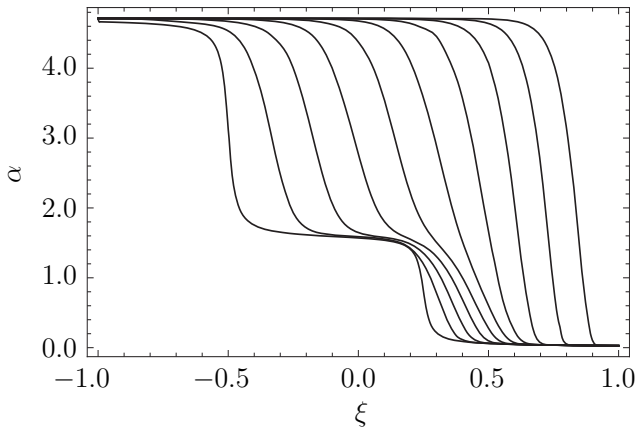

Figure 3: FEM solution of Eq. (6) with $w = 1.0$, $v = 2.0$ with an initial two-step configuration $\alpha(\xi, \tau = 0) = [\pi/2 - \arctan(50\xi + 25)] + [\pi/2 - \arctan(50\xi - 25/2)]/2$. The subsequent evolution of this profile is shown at intervals of $\Delta\tau = 0.025$. The velocity of the profiles at later times, corresponding to the solitary wave Eq. (16), fulfills Eq. (14) in the main text.

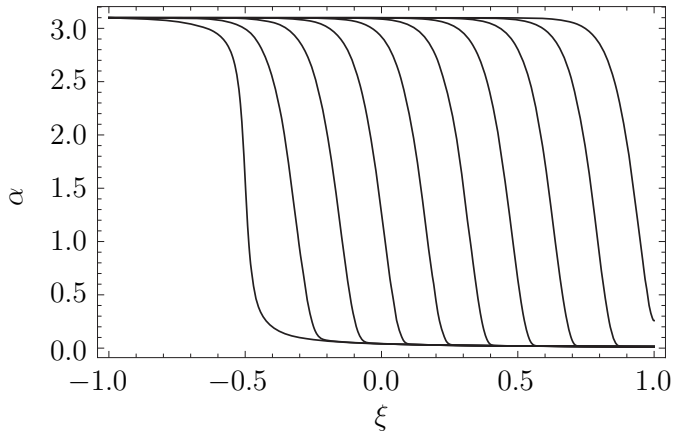

Figure 4: FEM solution of Eq. (6) with $w = 1.0$ and $v = 2.0$. The initial configuration is $\alpha(\xi, \tau = 0) = (\pi/2) - \arctan(50x - 25)$. The subsequent evolution of the profile is shown at intervals of $\Delta\tau = 0.05$. The velocity of the profiles, corresponding to the solitary wave Eq. (16), fulfills Eq. (14) in the main text.

terms of the variable z, as $\tau \to \pm\infty$. In these limits, the integration constant K defined in Eq. (12) becomes $K = U\alpha_\pm - v\alpha_\pm^2/2$, where we chose $\alpha_+ > \alpha_- \geq 0$ for the two asymptotic areas of the film and hence $U > 0$. Since $\alpha_\pm$ are real we conclude from Eq. (15) that $0 \leq K = v\alpha_+\alpha_-/2 < U^2/2v$. Eq. (12) can now be integrated in a straightforward manner, i.e.,

$$\sqrt{\alpha_-}\log\left(\frac{\sqrt{\alpha_s}+\sqrt{\alpha_-}}{\sqrt{\alpha_s}-\sqrt{\alpha_-}}\right) - \sqrt{\alpha_+}\log\left(\frac{\sqrt{\alpha_s}+\sqrt{\alpha_+}}{\sqrt{\alpha_+}-\sqrt{\alpha_s}}\right) = \frac{v}{2w}(\alpha_+ - \alpha_-)\,(z - 2z_0)\ , \qquad (16)$$

where z_0 constitutes the initial condition. We note that $\alpha_s \to \alpha_+$ as $\tau \to \infty$ and $\alpha_s \to \alpha_-$ as $\tau \to -\infty$ as long as the initial conditions are chosen such that $\alpha_+ > \alpha_s(z_0) > \alpha_-$. The left-hand side of Eq. (16) now describes a α_s-profile that is translated in time. With a given initial data $\alpha_s(z_0)$ the asymptotic values $\alpha_\pm$ are finite. It is a straightforward calculation to show that the solution α_s of the form Eq. (16) is stable for small deformations at large values of $|\xi|$. This follows from the observation that any solution $\alpha = \alpha_s + \delta$ of Eq. (6) leads to a diffusion equation for δ keeping terms to linear order in δ for large values of $|\xi|$.

We show in Fig. 3 a finite-element (FEM) solution to Eq. (6) for an initial arctan-profile with two steps. The figure shows the initial profile of α versus ξ and subsequent profiles at regular time intervals. We observe that the initial profile progressively deforms into a stable profile that moves at constant speed. This is the solitary wave α_s as given by Eq. (16). Indeed, the initial step to the left in Fig. 3 moves with larger velocity than that to the right, eventually overtaking and absorbing it. This is clear from Eq. (14), which shows that the velocity of a solitary wave is proportional to the average α to the left and to the right of it. This is generally true: As long as α to the far left is larger than the α to the far right, all deformations will be absorbed into a single solitary wave moving with the velocity given by Eq. (14). In other words, the solitary wave exhibits a topological stability. In Fig. 4 we show how an initial single-step configuration rapidly evolves into the stable solitary wave α_s.

In conclusion we have shown that the combined effects of non-linear convection and diffusion for the dynamics of a wetting film can lead to a rather intriguing physics which, in our case, can be analyzed exactly. The local dynamical equation used describes a balance between viscous and capillary forces at the interface between the wetting film and a bulk liquid. When the bulk flow rate drops to zero along a pore, perturbations of the film spread diffusively and this non-linear diffusivity may, as we have seen, lead to the appearance of shock fronts and, remarkably, to anomalous diffusion. In the presence of non-linear convection in addition to non-linear diffusion, we have seen the appearance of solitary waves. Numerical analysis has shown that the presence of several wave fronts eventually merges into a single solitary wave, the dynamical origin of which we have outlined. Concerning potential applications we, e.g., notice that drainage processes, where a less wetting fluid displaces a more wetting fluid in a porous medium, appears to be fairly well understood today. This is, however, not the case in the opposite situation which we describe, i.e. imbibition, where a more wetting fluid displaces a less wetting fluid. We have also observed that the dynamical equation considered also enters in the context of non-linear heat conduction where solitary waves therefore also may appear if a suitable form of convection is present.

This work has been supported by the Norwegian Research Council, EMGS AS, Numerical Rocks AS and StatoilHydro AS. One of the authors (B.-S.S.) wishes to thank Professor Frederik G. Scholtz for a generous hos-

pitality during a joint NIThePand Stias, Stellenbosch (S.A.), workshop in 2009 when the present work was in progress. The authors are grateful to referees for pointing out Refs.[15, 16]. During the submission process of the present paper a related work has appeared [18] with, however, a different focus then the issues discussed here.

[1] J. P. Bouchaud and A. Georges, Phys. Rep. **195**, 127 (1990); H. Scher, M. F. Schlesinger and J. T. Bendler, Phys. Today, **44** 1, 26 (1991); M. F. Schlesinger, G. M. Zaslavsky and J. Klafter, Nature, **363**, 31 (1993): S. Havlin and D. Ben-Avraham, Adv. Phys. **51**, 187 (2002).

[2] F. Mainardi, Chaos, Solitons & Fractals **7**, 1461 (1996); R. Metzler and J. Klafter, Phys. Rep. **339**, 1 (2000) and J. Phys. A**37**, R161 (2004).

[3] T. Kosztołowics, K. Dworecki, and St. Morówcyński, Phys. Rev. Lett. **94**, 170602 (2005); E. N. de Azevedo, P. L. de Sousa, R. E. de Souza, and M. Engelsberg, Phys. Rev. E **73**, 011204 (2006); E. N. de Azevedo, D. V. da Silva, R. E. de Souza, and M. Engelsberg, Phys. Rev. E **74**, 041108 (2006); J. C. Cressoni, M. A. A. da Silva, and G. M. Viswanathan, Phys. Rev. Lett. **98**, 070603 (2007); E. N. de Azevedo, L. R. Alme, M. Engelsberg, J. O. Fossum, and P. Dommersnes, Phys. Rev. E **78**, 066317 (2008).

[4] Ya. Zeldovich, and Yu. A. Raizer, *Physics of Shock Waves and High Temperature Hydrodynamic Phenomena* (Academic Press, New York, 1967).

[5] F. J. Mayer, J. F. McGrath, and J. W. Steele, J. Phys. A: Math. Gen. **16**, 3393 (1983).

[6] E. W. Washburn, Phys. Rev. **17**, 273 (1921); D. A. Nield, and A. Bejan, *Convection in Porous Media* (Springer Verlag, New York, 1992); P. A. Gauglitz, and C. J. Radke, J. Colloid and Interface Science **117**,14 (1990); J. A. Mann, L. A. Romero, R. R. Rye, and F. G. Yost, Phys. Rev. E, **52**, 3967 (1995); L. A. Romero and F. G. Yost, J. Fluid Mech. **322**, 109 (1996); A. R. Kovscek, and C. J. Radke, Coll. and Surf. **117**, 55 (1996); S. Gerdes, A. M. Cazabat, and G. Ström, Langmuir, **13**, 7258 (1997); E. Kim, and M. Whitesides, J. Phys. Chem. B **101**, 855 (1997); M. M. Weislogel, Phys. of Fluids **13**, 3101 (2001); P. B. Warren, Phys. Rev. E **69**, 041601 (2004); M. S. Al-Gharbi and M. J. Blunt, Phys. Rev. E **71**, 016308 (2005).

[7] C. Hall, Cement and Concrete Research, **37**, 378 (2007).

[8] G. B. Whitham, *Linear and Nonlinear Waves* (Wiley Interscience Publ., New York, 1974).

[9] S. Cathelin, J.-L. Gennisson, M. Tanter, and M. Flink, Phys. Rev. Lett. **91**, 164301 (2003).

[10] F. A. L. Dullien, *Porous Media: Fluid Transport and Pore Structure, Second Edition* (Academic Press, San Diego, 1992).

[11] M. Dong, and I. Chatiz, J. Colloid and Interface Science **172**, 278 (1995).

[12] H. Mori, Prog. Theor. Phys. **33** 423 (1965); **34**, 399 (1965); M. H. Lee, Phys. Rev. B **26**, 2547 (1982); J. Math. Phys. **24**, 2512 (1983); Phys. Rev. Lett. **85**, 2422 (2000).

[13] R. Morgado, F. A. Oliveira, G. G. Batrouni, and A. Hansen, Phys. Rev. Lett. **89**, 100601 (2002); B.-S. Skagerstam and A. Hansen, Europhys. Lett. **72**, 513 (2005).

[14] G. M. Schütz and S. Steffen, Phys. Rev. E **70**, 045101 (2004).

[15] C. Tsallis, , and D. J. Bukman, Phys. Rev. E **54**, R2197 (1996).

[16] N. Goldenfeld, O. Martin, Y. Oono, and F. Liu, Phys. Rev. Lett. **64**, 1361 (1990).

[17] J. Crank, *The Mathematics of Diffusion* (Oxford University Press, London, 1975).

[18] J. S. Andrade Jr., G. F. T. da Silva, A. A. Moreira, F. D. Nobre, and E. M. F. Curadao, arXiv:1008.1221 (cond-math.stat-mech) (2010).